

## CARBON-OXYGEN WHITE DWARF ACCRETING CO-RICH MATTER. II. SELF-REGULATING ACCRETION PROCESS UP TO THE EXPLOSIVE STAGE

LUCIANO PIERSANTI

Osservatorio Astronomico di Teramo, Via M. Maggini 47, 64100 Teramo, Italy;  
piersanti@te.astro.it

SIMONA GAGLIARDI<sup>1</sup>

Università degli Studi Roma Tre, via della Vasca Navale, 84, 00146 Rome, Italy;  
gagliardi@astrte.te.astro.it

ICKO IBEN, JR.

Astronomy Department, University of Illinois, 1002 West Green Street, Urbana, IL 61801;  
icko@astro.uiuc.edu

AND

AMEDEO TORNAMBÉ

Osservatorio Astronomico di Teramo, Via M. Maggini 47, 64100 Teramo, Italy;  
tornambe@astrte.te.astro.it

Received 2003 June 19; accepted 2003 August 6

### ABSTRACT

We investigate the effect of rotation on the evolution of double-degenerate white dwarf systems, which are possible progenitors of Type Ia supernovae. We assume that prior to merging, the two white dwarfs rotate synchronously at the orbital frequency and that in the merger process, the lighter white dwarf is transformed into a thick disk from which the more massive white dwarf initially accretes at a very high rate ( $\sim 10^{-5} M_{\odot} \text{ yr}^{-1}$ ). Because of the lifting effect of rotation, the accreting white dwarf expands until the gravitational acceleration and centripetal acceleration required for binding at the surface become equal, initiating a Roche instability. The white dwarf continues to accrete matter from the disk, but at a rate that is determined by the balance between two competing processes operating in outer layers: (1) heating, expansion, and spin-up due to accretion and (2) cooling and contraction due to thermal diffusion. The balance produces an accretion rate such that the angular velocity of the white dwarf  $\omega_{\text{WD}}$  and the break-up angular velocity  $\omega_{\text{cr}}$  remain equal. Because of the deposition of angular momentum by accreted matter and the contraction of the accreting star,  $\omega_{\text{WD}}$  increases continuously until the rotational energy reaches about 14% of the gravitational binding energy; then, another instability sets in: the structure is forced to adopt an elliptical shape and emit gravitational waves. Thereafter, a balance between the rate of deposition of angular momentum by accreted matter and the rate of loss of angular momentum by gravitational waves produces a nearly constant or “plateau” accretion rate of  $\sim 4 \times 10^{-7} M_{\odot} \text{ yr}^{-1}$ . The mass of the accreting white dwarf can increase up to and beyond the Chandrasekhar mass limit for nonrotating white dwarfs before carbon ignition occurs. Independent of the initial value of the accretion rate, the physical conditions suitable for carbon ignition are achieved at the center of the accreting white dwarf and, because of the high electron degeneracy, the final outcome is an event of SN Ia proportions. Our results apply to merged binary white dwarf systems which, at the onset of explosive carbon ignition, have a total mass in the range 1.4–1.5  $M_{\odot}$ .

*Subject headings:* accretion, accretion disks — stars: rotation — supernovae: general — white dwarfs

### 1. INTRODUCTION

In spite of their pivotal role both in observational cosmology and in the chemical evolution of matter in the universe, Type Ia supernovae (SNe Ia) are still not fully understood as a phenomenological class. In particular, no clear consensus exists about either the stellar progenitors of these events or the details of the explosion mechanism.

The observational evidence can be interpreted to suggest that the progenitor systems of SNe Ia are carbon-oxygen (CO) white dwarfs (WDs) that accrete matter from their companions in binary systems. The longevity of progenitors, at least in elliptical galaxies, is one of the major indicators that binary systems are involved. If the mass of

the accreting star can attain the Chandrasekhar limit ( $M_{\text{Ch}}$ ), central carbon burning is ignited under highly electron-degenerate conditions, thus producing an explosion. First proposed by Hoyle & Fowler (1960), white dwarf explosions explain several observational properties of SNe Ia, including the energetics, the nucleosynthetic products in the spectrum, and the light curve, and such explosions are widely accepted as the mechanism responsible for SNe Ia. However, there is as yet no consensus on the precise nature of the companion in the binary system and on the physical properties of the burning front during the explosion (for a recent review see Hillebrandt & Niemeyer 2000).

In part because it is amenable to spherically symmetric calculations, the most commonly explored scenario for the progenitor system is the so-called single-degenerate (SD) scenario: the binary system consists of a CO WD and a low-mass main-sequence or red giant star. The first concrete

<sup>1</sup> Osservatorio Astronomico di Teramo, Via M. Maggini 47, 64100 Teramo, Italy.

SD progenitor system proposed consists of an intermediate mass component that evolves into a CO white dwarf and a low-mass companion that evolves into a red giant that, on filling its Roche lobe, transfers matter to the white dwarf (Whelan & Iben 1973). In this scenario, the accreted hydrogen-rich matter is burned first into helium and then into carbon and oxygen. If the ram pressure of the wind emitted by the accretor remains smaller than the ram pressure of the accretion stream, and if the helium produced by hydrogen burning can be converted relatively quiescently into carbon and oxygen, the underlying white dwarf can grow in mass until it reaches the Chandrasekhar mass and then explodes (Hachisu, Kato, & Nomoto 1996). However, numerical explorations (Cassisi, Iben, & Tornambé 1998; Piersanti, Cassisi, Iben, & Tornambé 1999, 2000; and Piersanti, Cassisi, & Tornambé 2001) suggest that the helium shell flash, which occurs when the helium layer built up by hydrogen burning reaches a critical mass, is very violent (see also Iben & Tutukov 1991). Even if the flash is not dynamical, it is sufficiently energetic to force the expansion of the entire helium layer and of overlying hydrogen-rich matter into a common envelope of giant dimensions, which contains both stars in the binary system. The eggbeater frictional interaction between the binary components and common envelope material drives off the expanded material, most of which is lost from the system. If, on the other hand, the helium flash is dynamical, the explosive event delivers energy comparable to that of an observed SN Ia (Nomoto 1982a, 1982b), but the ejectum of such an event contains much more unburned helium and iron peak elements than has ever been detected spectroscopically (Woosley & Weaver 1994).

The alternate so-called double-degenerate (DD) scenario supposes that the immediate progenitor of the SN Ia is a binary system composed of two CO WDs with total mass of the order of or greater than  $M_{\text{Ch}}$  and with an initial orbital separation such that the merging of the two components due to orbital angular momentum loss by gravitational wave radiation (GWR) occurs on a timescale smaller than the Hubble time (Iben & Tutukov 1984a, 1984b; Webbink 1984). Numerical simulations by Benz et al. (1990) and by Rasio & Shapiro (1995) confirm that, at the merging stage, the less massive Roche lobe-filling white dwarf undergoes mass loss on a dynamic timescale, disrupting itself completely and forming an accretion disk around the more massive WD (Tutukov & Yungelson 1979). Thereafter, CO-rich matter is accreted onto the WD from the disk. This scenario explains in a very simple fashion the absence of Balmer lines in SNe Ia spectra and provides a very natural way for the accreting WD to attain the Chandrasekhar mass limit without encountering the road block of a helium shell flash. Nevertheless, the observational search for DD systems that could be progenitors of SNe Ia has not as yet provided “smoking gun” candidates (Robinson & Shafter 1987; Bragaglia et al. 1990; Saffer, Livio, & Yungelson 1998), although recently one potential candidate has been detected (KPD 0422+5421, see Koen, Orosz, & Wade 1998).

Another possible shortcoming of the DD scenario is that central explosive carbon burning can be ignited only if the effective accretion rate onto the WD is smaller than  $\sim 10^{-6} M_{\odot} \text{ yr}^{-1}$  (Nomoto & Iben 1985; Saio & Nomoto 1985, 1998; Piersanti, Gagliardi, Iben, & Tornambé 2003, hereafter Paper I). However, after a merger, the effective accretion rate onto the more massive WD could be as large as the

Eddington limit ( $\sim 10^{-5} M_{\odot} \text{ yr}^{-1}$ ), with the result that carbon burning is ignited off center well before the mass of the accreting WD reaches  $M_{\text{Ch}}$ . In this event, the penultimate outcome is an oxygen-neon-magnesium (ONeMg) WD, not a SN Ia event (Saio & Nomoto 1985, 1998): continued accretion presumably leads to the collapse of the ONeMg WD into a neutron star (Isern et al. 1983; Hernanz et al. 1988).

Almost all results concerning the direct deposition of CO-rich matter onto WDs have been obtained by assuming that rotation is negligible in the evolution of the accreting structure. This assumption, which is, in general, well founded and supported by the observational evidence for single stars, is not valid for WDs in DD systems. For, in such systems, because of microviscosity in the presence of even a small magnetic field, the two evolved components interact tidally on a timescale shorter than the GWR timescale in such a way that, by the time merger occurs, each component rotates around its own center of mass with the same angular velocity as its center of mass rotates around the center of mass of the binary system. That is, at the merger, the WDs rotate with an angular velocity equal to the orbital Keplerian angular velocity. It follows that, immediately after the merger occurs, the angular velocity of the central WD is large enough that the effect of rotation must be taken into account in modeling the consequences of the subsequent accretion process.

In Paper I we analyzed systematically the effect of rotation on the evolution of accreting WDs as a function of the initial angular velocity of the WD, the angular momentum deposited by the accreted matter, and the accretion rate. The results obtained (see Figs. 14 and 18 in Paper I) show that, for a fixed value of  $\dot{M}$ , the larger the initial angular velocity of the WDs, the larger is the expansion of the surface layers produced by the conversion of gravitational energy into heat. The value of the gravitational acceleration at the surface decreases, and when it becomes equal to the centripetal acceleration required for binding to the surface, the Roche instability occurs and the accretion process is interrupted. The expansion of the outer layers is due to an overpressure produced by the conversion of the gravitational energy of accreted matter into heat and the approach to the instability is accelerated by the spinning-up of the WD due to the deposition of angular momentum by accreted matter.

On the basis of these results, we can argue that, for DD systems that undergo a merger, CO-rich matter is accreted at a very high rate ( $\sim 10^{-5} M_{\odot} \text{ yr}^{-1}$ ) onto the more massive component until it rotates with an angular velocity of the order of  $0.1 \text{ rad s}^{-1}$  and the Roche instability sets in. This occurs when just a small percentage of the matter from the thick disk has been deposited, the exact amount depending on both the accretion rate and the initial angular velocity. In the conclusion of Paper I, we suggest that the occurrence of the Roche instability does not imply that the accretion process comes to an end, but only that the rate at which matter is deposited must decrease. We observe that, if  $\dot{M}$  is reduced, angular momentum is added at a smaller rate to the WD, so that it spins up more slowly. In addition, lowering  $\dot{M}$ , the rate at which gravitational energy is delivered decreases and the surface layers stop expanding and begin to contract, thus producing an increase in the local value of the gravitational acceleration.

To verify this conjecture, in the present work we analyze further the evolution of a DD system, taking into account the effect of rotation on both the thermal evolution of the accreting WD and the rate at which matter is effectively deposited onto the star. This work is organized as follows: in § 2, we present the evolution of a selected DD system during the premerging phase; in § 3, we discuss the evolution of the WD during the accretion process; and in § 4, we provide a summary.

The input physics as well as the evolutionary code we use in the present work are the same as in Paper I (see § 2); the technique adopted for including the effect of rotation is the same as discussed in § 5 of that paper.

## 2. EVOLUTION DURING THE GWR-DRIVEN SHRINKING PHASE

We consider a DD system composed of two CO WDs with masses  $M_1 = 0.8 M_\odot$  and  $M_2 = 0.75 M_\odot$ , respectively, at a separation  $A = 0.9 R_\odot$ . Such a system can form as a consequence of two common envelope episodes in an original binary system consisting of two stars with masses in the range  $6\text{--}8 M_\odot$  at an initial separation in the range  $10\text{--}50 R_\odot$  (see Iben & Tutukov 1984b; Tornambé 1989). As is well known, DD binary systems shrink because of orbital angular momentum loss by GWR: since both components are rotating around the center of mass of the system along stable orbits, the system itself has a quadrupole moment, and, in consequence, angular momentum and rotational energy are lost because of GWR, thus inducing the two components to become closer. The merging timescale is determined by the efficiency of angular momentum loss by GWR, and this efficiency depends on the initial orbital parameters of the system, mainly on the separation  $A$ . The value we have chosen for the separation guarantees that the merger of the two components occurs in a time on the order of  $\sim 10^8$  yr.

Whether or not tidal forces can act to spin up the white dwarfs during the premerger stage depends on whether or not the microscopic viscosity of electron-degenerate matter is effective in trapping tidal energy (Webbink & Iben 1988; Iben, Tutukov, & Fedorova 1998). Although a satisfactory quantitative theory of the viscosity of electron-degenerate matter is lacking, it is known that if even a small magnetic field with a proper orientation exists, viscosity may be high enough (Sutantyo 1974) to ensure that the synchronization timescale is smaller than the GWR timescale (see the discussion in Iben, Tutukov, & Fedorova 1998). In our computations, we have assumed that the viscosity is large enough that the white dwarf rotation rates are quickly synchronized at the orbital frequency. Because of viscous dissipation, the tidal forces also cause the interiors of the WDs to heat up, leading to an increase of their surface luminosity to the extent that the detection probability of the systems at optical wavelengths increases tremendously (Iben, Tutukov, & Fedorova 1998). Partial and complete occultations of both components of duration in the range  $0.5\text{--}2'$  are expected. Both the tidal heating mediated by viscosity and the continuous increase of the angular velocity due to the shrinkage of the system affect the surface radii of the two components. In particular, because of tidal interactions that produce both the heating and the spin-up of the two stars, the WDs expand in such a way that the merging time is about 20% shorter than when rotation is neglected. Following Iben,

Tutukov, & Fedorova (1998), we have assumed that thermal energy is delivered in each mass shell at the same rate at which rotational energy is delivered; that is, we set  $\varepsilon_{\text{th}} = \varepsilon_{\text{rot}} = \frac{2}{3} R^2 \omega (d\omega/dt)$ . Because WDs are very compact, almost chemically homogeneous objects, we have also assumed that the redistribution of angular momentum occurs on such a short timescale that the accreting star can be regarded as a rigid rotator. On the other hand, the tidal energy delivered during the merging process is redistributed through the structures by thermal diffusion and, hence, the temperature profiles are determined by the local value of the thermal diffusion timescale ( $\tau_{\text{diff}}$ ) and must be calculated.

In our computations, the primary component has the same physical and chemical properties as the  $0.8 M_\odot$  WD described in Paper I (see § 3.1). During the GWR shrinking phase, we have followed in detail the evolution of the primary component by including both the spin-up and the heating due to tidal interactions. The initial structure of the secondary has been obtained by evolving a pure helium star from the helium main sequence up to the WD cooling sequence. Thereafter, we have assumed that the secondary evolves homologously with the primary.

The thermal evolution of the primary during the orbital shrinking phase is reported in Figure 1, where temperature profiles for several selected structures are plotted. At first, the WD remains nearly isothermal, cooling uniformly from  $\log(T) \sim 7$  to  $\log(T) \sim 6.9$ . Both radiative losses from the surface and the energy required to expand matter locally in response to spin-up contribute to the cooling. When the release of tidal energy locally through viscous friction becomes dominant, the structure heats up. The formation of a maximum in temperature in the outer layers (at the mass coordinate  $M \sim 0.75 M_\odot$ ) is, in part, due to the adopted law for releasing tidal energy locally and to the fact that the thermal diffusion timescale is longer than the timescale for angular momentum loss by GWR.

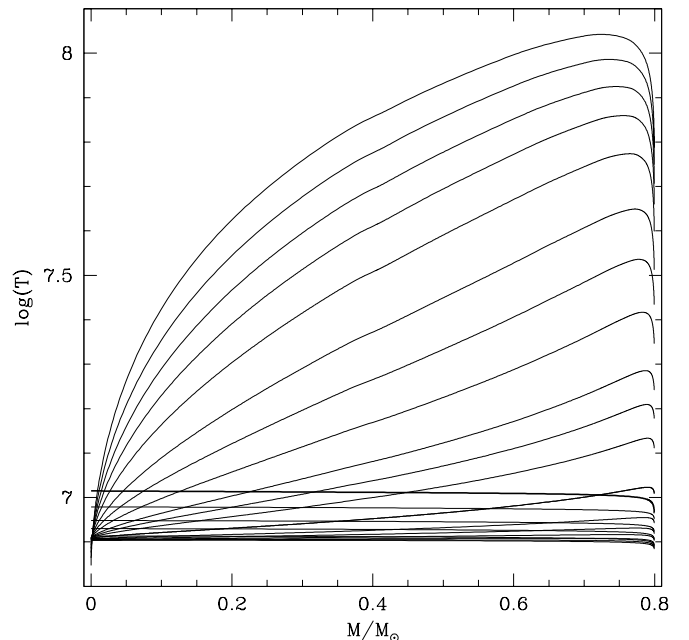


FIG. 1.—Temperature profiles for some selected structures during the premerging phase of the primary component ( $M_1 = 0.8 M_\odot$ ). *Bold line* at  $T \sim 10^7$  K: First model (see text).

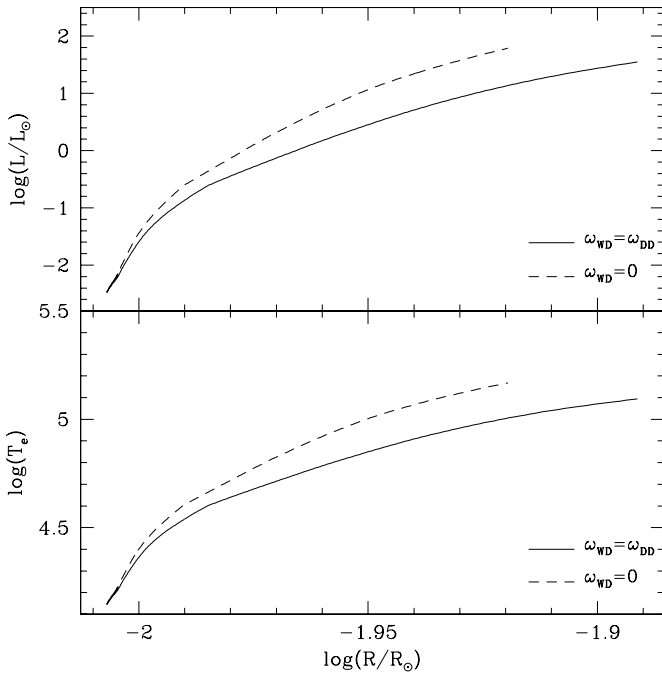


FIG. 2.—Evolution of the effective temperature (*lower panel*) and of the surface luminosity (*upper panel*) as functions of the surface radius of the primary component of the DD system during the premerger phase. *Solid lines*: Rotating systems. *Dashed lines*: Nonrotating systems.

Prior to merger, the luminosity of the primary component increases from  $1.38 \times 10^{-3}$  to  $35.48 L_{\odot}$ , a (bolometric) brightening by  $\sim 11$  mag. If the orbital plane is in the line of sight of an observer, the occultation period just before merger is of the order of  $70''$ . The merger of the two WDs occurs after  $1.1863 \times 10^8$  yr, and at this stage, the angular velocity of the system is  $\omega_0 = 0.177$  rad  $s^{-1}$ .

The inclusion of the lifting effect of rotation on the thermal evolution of the shrinking WDs affects their physical properties at the moment of contact, as depicted in Figure 2, where we report the evolution of the total luminosity (*upper panel*) and of the effective temperature (*lower panel*) of the primary component as functions of the surface radius of the primary. If the lifting effect of rotation is not included (*dashed lines*), both components remain smaller (hotter at the surface) and more luminous, and the merger occurs later than when the effects of rotational lifting are included. At the merging time, the orbital angular velocity of the system without the lifting effect is larger by about 10% than the orbital angular velocity of the system with the lifting effect included.

### 3. THE ACCRETION PHASE

#### 3.1. Evolution up to the Roche Instability

Calculations of the dynamical evolution of close WDs (Benz et al. 1990; Rasio & Shapiro 1995) show that the merging process produces a compact core, which is the original primary component, surrounded by a thick disk, which is composed of the matter of the secondary and rotates with the Keplerian angular velocity. In our simulations, we assume that the disk is at all times in contact with the core, so that its angular velocity  $\omega_D$  at the point of contact coincides with  $\omega_{WD, cr}$ , the Keplerian angular velocity of the

outer layers of the accreting WD core. Because of the loss of angular momentum, matter flows from the disk to the WD. The accreted matter carries a specific angular momentum given by  $j_D = \dot{M} \omega_D R_s^2 = \dot{M} (GMR_s)^{1/2}$ , where  $R_s$  is the surface radius of the accreting star and  $M$  is its mass.

The rate at which matter is accreted depends on the rate of angular momentum loss from the disk. There are currently no clear indications as to precisely what the initial value of  $\dot{M}$  should be, but it seems reasonable to assume that it is of the order of the Eddington limit (see discussions in Nomoto & Iben 1985 and Saio & Nomoto 1985). In the present work, we adopt an initial accretion rate of  $\dot{M} = 8 \times 10^{-6} M_{\odot} \text{ yr}^{-1}$ . Fortunately, it turns out that the main characteristics of the subsequent evolution are independent of the value adopted for the initial rate.

Standard nonrotating models that accrete CO-rich matter at the adopted rate ignite carbon burning off-center when the total mass of the WD is of the order of  $1.1 M_{\odot}$  (see § 3.2 in Paper I). The penultimate outcome is an ONeMg WD, which, after accreting another  $0.3 M_{\odot}$ , explodes as a core-collapse supernova (see Isern et al. 1983; Hernanz et al. 1988).

As discussed in Paper I, when the lifting effect of rotation is taken into account, a new phenomenon comes into play: the Roche instability. This instability occurs when the gravitational acceleration at the surface becomes smaller than the centripetal acceleration needed for binding to the surface; the outer layers of the WD become unbound and matter can no longer be accreted at an arbitrary (the initially adopted) rate. During the evolution that leads up to the onset of this instability, the gravitational potential energy liberated by accreted matter is converted into heat more rapidly than it can be removed by thermal diffusion (the local value of the thermal diffusion timescale is larger than the compressional heating timescale,  $\tau_{ch}$ ). As a consequence, local heating produces an overpressure that expands the surface layers. Thus, at the surface, the gravitational acceleration and, hence, the critical angular velocity  $\omega_{cr}$  decrease. On the other hand, the WD angular velocity  $\omega_{WD}$  continues to increase due to the deposition of angular momentum by the accreted matter. This situation is depicted in Figure 3, where we report the evolution of  $\omega_{WD}$  (*solid line*) and of  $\omega_{cr}$  (*dashed line*). The Roche instability sets in when only a small amount of matter ( $\sim 0.034 M_{\odot}$  in the case at hand) has been transferred from the disk to the central white dwarf.

#### 3.2. The Self-Regulating Accretion Phase

Once the Roche instability has been encountered, the rate of accretion is determined by the condition that  $\omega_{WD} \leq \omega_{cr}$ . One can think of the ensuing evolution as being controlled by the simultaneous operation of two competing processes. When  $\omega_{WD} = \omega_{cr}$ , accretion cannot occur. Because of the inward diffusion of heat, the overpressure in outer layers of the WD decreases; these layers contract and the WD spins up slightly. The moment of inertia of the WD can be written as  $I = I_0 + \Delta I$ , where  $I_0 = \alpha M_0 r_0^2$  is the contribution of inner layers,  $\Delta I = \beta \Delta M r_{WD}^2$  is the contribution of outer layers, and  $M_0 + \Delta M = M_{WD}$ , where  $\Delta M \ll M_0$ . Assuming that  $\alpha$  and  $\beta$  may be treated as constants, we have from the conservation of angular momentum that

$$\frac{\delta \omega_{WD}}{\omega_{WD}} = -\frac{\delta I}{I} = -2 \frac{\delta r_{WD}}{r_{WD}} \frac{I_0}{I} \left( \frac{\delta r_0 / r_0}{\delta r_{WD} / r_{WD}} \right) + \frac{\Delta I}{I}, \quad (1)$$

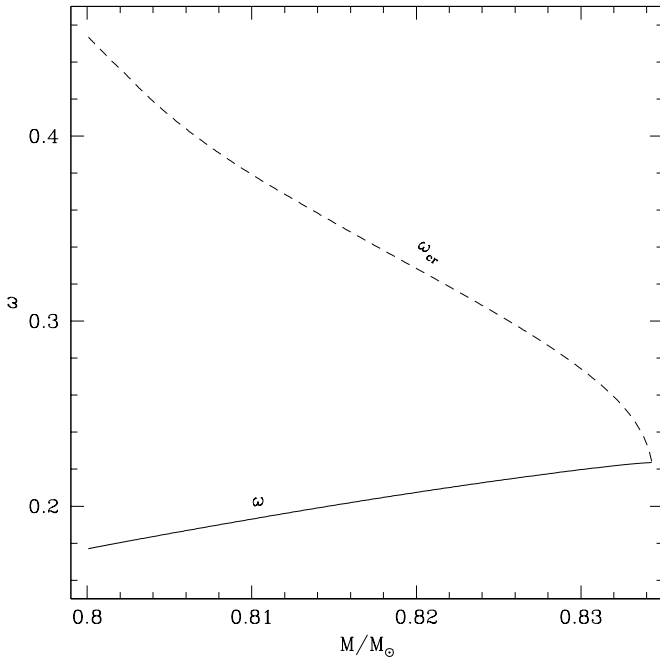


FIG. 3.—Evolution of the angular velocity of the accreting WD  $\omega_{WD}$  (solid line) compared with the value of the critical angular velocity  $\omega_{cr}$  at the surface (dashed line).

where  $\delta q$  denotes the change with time in the quantity  $q$ . We note that  $I_0/I < 1$ , and that, since the degree of expansion or shrinkage  $|\delta r_0/r_0|$  of the highly electron-degenerate inner layers is significantly smaller than the degree of shrinkage  $|\delta r_{WD}/r_{WD}|$  of the less electron-degenerate outer layers (the weaker the degeneracy, the more pressure depends on the temperature), the first term in the coefficient of  $-2(\delta r_{WD}/r_{WD})$  in equation (1) is small compared with unity and may be neglected. Since  $\Delta M/M_{WD}$  is small compared with unity and  $r_0/r_{WD}$  is of the order of unity,  $\Delta I/I$  might be expected to be sufficiently smaller than unity that the effective coefficient of  $-\delta r_{WD}/r_{WD}$  in equation (1) is less than unity. On the other hand, the critical angular velocity changes according to  $\delta \omega_{cr}/\omega_{cr} = -\frac{3}{2}(\delta r_{WD}/r_{WD})$ . Thus, when accretion ceases, outer layers contract and  $\omega_{cr}$  increases more rapidly than does  $\omega_{WD}$ ; instantaneously,  $\omega_{WD} < \omega_{cr}$ . Hence, accretion resumes, and because of the deposition of angular momentum by the accreted matter, the WD continues to spin up. Because of accretion-induced heating, the outer layers expand and  $\omega_{cr}$  decreases; once again,  $\omega_{WD}$  becomes equal to  $\omega_{cr}$  and accretion ceases. The cycle repeats. In reality, the two processes occur at the same time, and the balance between the two determines the actual rate at which the WD accretes and whether, as it spins up continuously, its radius increases or decreases.

In order to estimate this balance, we make use of the fact (found by experiment) that, in response to the removal of a discrete amount of matter (along with the associated angular momentum), a model WD readjusts to a new equilibrium configuration at larger  $\omega_{WD}$  on a timescale that is small compared with the accretion timescale. The white dwarf shrinks slightly and spins up. In accordance with the argument in the previous paragraph,  $\omega_{cr}$  increases more rapidly than  $\omega_{WD}$ , which remains almost constant, demonstrating that the coefficient of  $-\delta r_{WD}/r_{WD}$  in equation (1) is indeed less than unity. The algorithm we have adopted has two

components: (1) continuous accretion at the rate  $\dot{M} = 8 \times 10^{-6} M_{\odot} \text{ yr}^{-1}$ , and (2) removal, at discrete intervals, of enough matter to meet the criterion  $\omega_{WD} < \omega_{cr}$ . Thus, we have assumed that each phase of steady accretion, accompanied by heating and expansion of outer layers and overall spin-down is interrupted by an instantaneous loss of mass followed by a short-lived phase of cooling and contraction of outer layers and overall spin-up during which accretion continues at the adopted rate. The matter returned to the disk is assumed to have a specific angular momentum equal to that of the accretion disk ( $j_D$ ). We emphasize that our algorithm is one of convenience only. In reality, the flow of matter and angular momentum is irreversibly from the disk to the white dwarf; the white dwarf does not return these quantities to the disk.

The adopted algorithm gives the results reported in Figure 4, where (a) shows that, after an initial discontinuous drop, the rate ( $\dot{M}_{eff}$ ) at which matter is effectively deposited

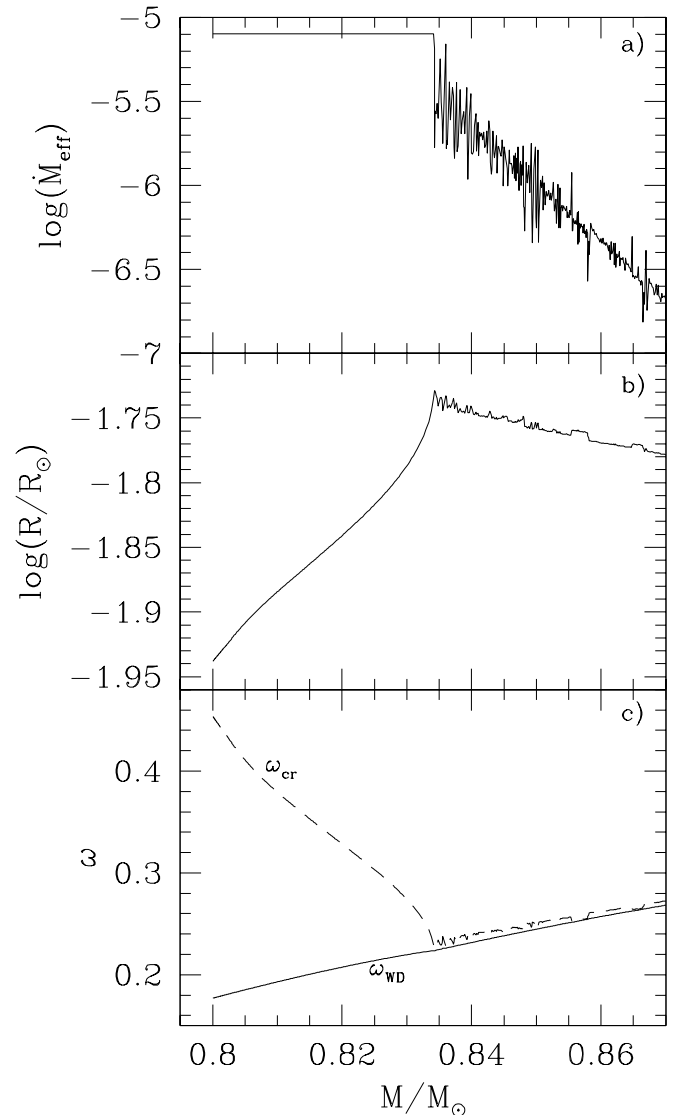


FIG. 4.—Evolution of some physical parameters before and after the occurrence of the Roche instability:  $\dot{M}$  (in units of  $M_{\odot} \text{ yr}^{-1}$ ) in (a), surface radius (in solar units) in (b), and angular velocities (in  $\text{rad s}^{-1}$ ) in (c).  $\omega_{WD}$  is the white dwarf angular velocity and  $\omega_{cr}$  is the critical angular velocity (see text).

onto the WD decreases steadily with time. The evolution of the surface radius is shown in Figure 4b and  $\omega_{\text{WD}}$  and  $\omega_{\text{cr}}$  are shown in Figure 4c. It is interesting that in the balance between the two competing processes discussed at the beginning of this section, the tendency toward shrinkage (which must win when there is no accretion) prevails over the tendency toward expansion (which, as shown in Fig. 4b for  $M_{\text{WD}} < 0.834 M_{\odot}$ , wins when the accretion rate is high).

Were it not for the intervention of additional physical processes to stem the rate of decline in  $\dot{M}_{\text{eff}}$ , a time much longer than the Hubble time would be required for the mass of the accreting WD to reach the Chandrasekhar mass limit.

### 3.3. The GWR-driven Accretion Phase

Because of both the contraction of the outer layers and the deposition of angular momentum, the rotational energy of the WD increases with time, and the possibility must be entertained that other secular instabilities with permanent consequences can occur. Rotation tends to deform equipotential surfaces into elliptical shapes, but meridional circulations redistribute angular momentum in such a way as to restore cylindrical symmetry (Tassoul 1978). Furthermore, given the fact that our WD model is a variable density rigid rotator, neither the Solberg nor the Goldreich-Schubert-Fricke instabilities occur (Tassoul 1978). However, as discussed by Chandrasekhar (1970), when its rotational energy  $E_{\text{rot}}$  becomes a sufficiently large fraction of its gravitational binding energy  $E_g$ , a Maclaurin spheroid (which our models approximate) becomes secularly unstable to a deformation into a triaxial Jacobi ellipsoid. Since it possesses a quadrupole moment, such an ellipsoid emits GWR.

The critical value of the ratio  $\gamma = (E_{\text{rot}}/E_g)$  has been determined to be  $\gamma_{\text{cr}} \sim 0.14$  (Friedman & Schutz 1975). During the early, constant- $\dot{M}$  accretion phase of our model,  $\gamma$  remains small compared with  $\gamma_{\text{cr}}$ , since the angular velocity and, hence, the rotational energy, are relatively small. After the Roche instability has occurred,  $\gamma$  can be regarded as a measure of the deviation of the moment of inertia of the structure from that of a constant-density sphere. That is, since  $\omega_{\text{WD}} = \omega_{\text{cr}}$ , we can write

$$\gamma = \frac{E_{\text{rot}}}{E_g} = \frac{(1/2)I\omega_{\text{cr}}^2}{(1/2)(GM^2/R)} = \frac{2}{5} \frac{I}{I_{\text{sp}}}, \quad (2)$$

where  $I$  is the actual moment of inertia of the accreting structure and  $I_{\text{sp}}$  is the moment of inertia of a constant-density sphere of the same mass and radius as the accreting structure. Note that  $I_{\text{sp}}$  is an upper limit for the moment of inertia of a spherical object in which density increases inward.

During the self-regulating accretion phase, the WD becomes more compact and, because it also becomes less centrally condensed, its moment of inertia becomes closer to that of a constant-density sphere. This situation is depicted in Figure 5, where we report the time evolution of  $\gamma$  (Fig. 5a, *solid curve*) and of the logarithm of  $I$ , the moment of inertia of the accreting WD (Fig. 5b, *solid curve*). The dashed curves in these panels are, respectively, the critical value of  $\gamma$ ,  $\gamma_{\text{cr}}$  (Fig. 5a), and the logarithm of  $I_{\text{sp}}$  (Fig. 5b). The break in the slope of  $\gamma$  at  $M_{\text{WD}} \sim 0.834 M_{\odot}$  occurs when the Roche instability sets in and equation (2) becomes applicable;  $I/I_{\text{sp}}$  increases with time and  $\gamma$  becomes equal to  $\gamma_{\text{cr}}$  when  $M_{\text{WD}} \sim 0.865 M_{\odot}$ .

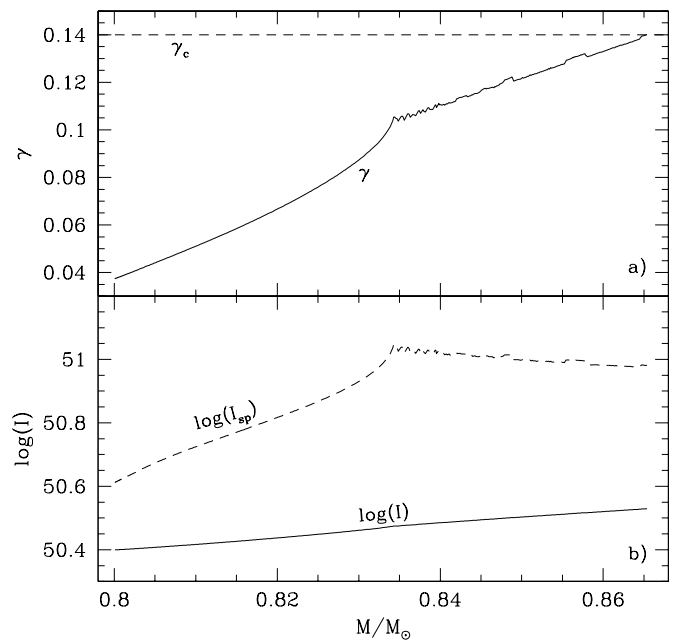


FIG. 5.—(a) Time evolution of  $\gamma$  (*solid curve*) and of  $\gamma_{\text{cr}}$  (*dashed curve*). (b) Evolution of the moment of inertia of the accreting WD (*solid line*) and that of a homogeneous sphere of the same mass and radius (*dashed line*). The break in the slope of  $\gamma$  occurs when the Roche instability sets in and, thereafter,  $\omega_{\text{WD}} = \omega_{\text{cr}}$ .

As angular momentum is removed from the WD, the value of the centripetal force required for binding at the surface decreases and the effective gravity increases; the WD structure therefore experiences a contraction and spins up in such a way that  $\gamma$  remains close to  $\gamma_{\text{cr}}$ . This means that GWR braking can be active for a long time.

The rate of angular momentum loss by GWR can be approximated by

$$\frac{dJ}{dt} = -J_0 \frac{1}{\tau_{\text{GWR}}} e^{-t/\tau_{\text{GWR}}}, \quad (3)$$

where  $J_0$  is the angular momentum of the WD when GWR begins and  $\tau_{\text{GWR}}$  is the timescale on which angular momentum braking due to GWR takes place. This timescale depends on the shape of the accreting WD and on its rotational energy. Following Chandrasekhar (1970) and Friedman & Schutz (1975), we assume that

$$\tau_{\text{GWR}}(\text{s}) \sim 10^{-8} \left[ \frac{c}{R(\gamma - \gamma_{\text{cr}})} \right]^5 \frac{1}{\omega^6}, \quad (4)$$

where  $R$  is the radius of the WD,  $c$  is the velocity of light, and  $\tau$  is given in seconds. It is clear that the more the WD structure deviates from spherical symmetry, the greater is the efficiency of angular momentum loss by GWR.

The evolution of several quantities during the two phases of self-regulated accretion is shown in Figure 6 as a function of  $M_{\text{WD}}$ . The effective accretion rate is shown in Figure 6a, the surface radius in Figure 6b, the ratio  $\gamma$  in Figure 6c, and the GWR timescale  $\tau_{\text{GWR}}$  in Figure 6d. When the secular instability is first encountered,  $\tau_{\text{GWR}}$  is very large and the efficiency of GWR braking is small. However, as the deformation into a triaxial shape progresses,  $\tau_{\text{GWR}}$  decreases, and GWR braking becomes the leading mechanism controlling the effective rate of accretion onto the WD. In particular,

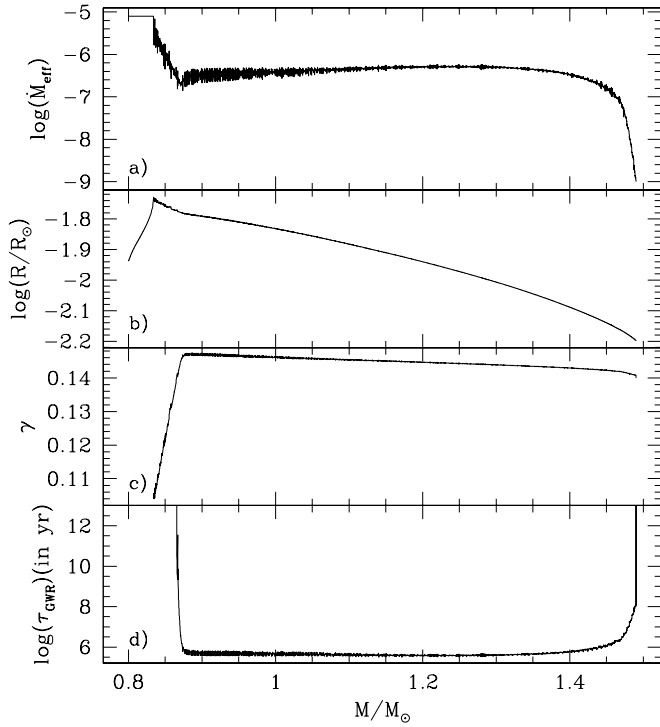


FIG. 6.—Time evolution of the effective accretion rate (a), the surface radius (b), the  $\gamma$  parameter (c), and the GWR timescale (d) (see text).

when  $M_{\text{WD}}$  exceeds  $\sim 0.87 M_{\odot}$ ,  $\tau_{\text{GWR}}$  remains smaller than  $10^6$  yr, and accretion proceeds at a nearly constant, plateau rate of  $\dot{M}_{\text{eff}} \sim 4 \times 10^{-7} M_{\odot} \text{ yr}^{-1}$  as the WD grows significantly in mass. At first, the accretion rate increases modestly; it then decreases modestly as the mass of the WD approaches and then exceeds the limiting mass for a nonrotating WD.

Eventually, the decrease in the rate of accretion accelerates as the excess rotational energy and angular momentum responsible for maintaining the Jacobian ellipsoid structure are depleted. The quadrupole moment of the WD structure decreases dramatically and both the rate of angular momentum loss by GWR and the effective rate of mass loss decline together.

### 3.4. Final System

Ultimately, secular stability is restored; the WD once again becomes a MacLaurin spheroid, GWR ceases, and accretion drops precipitously. The thermal energy excess that has been maintained by the conversion of gravitational potential energy into heat in exterior layers diffuses inward and the WD structure becomes essentially isothermal.

The thermal history of the WD during the phase of GWR-regulated accretion is described by the temperature profiles in Figure 7. The variable along the horizontal axis in this figure is the mass fraction  $M(r)/M_{\text{WD}}$ , with the WD mass relevant for each panel being indicated in the panel. Figures 7a and 7b show temperature profiles at, respectively, the onset of the Roche instability and the onset of the secular instability. The pronounced bump in the profile in Figure 7a reveals the thermal energy excess produced by a relatively large accretion rate; the less pronounced bump in the profile of Figure 7b reflects the smaller accretion rate near the beginning of the GWR-regulated phase of accre-

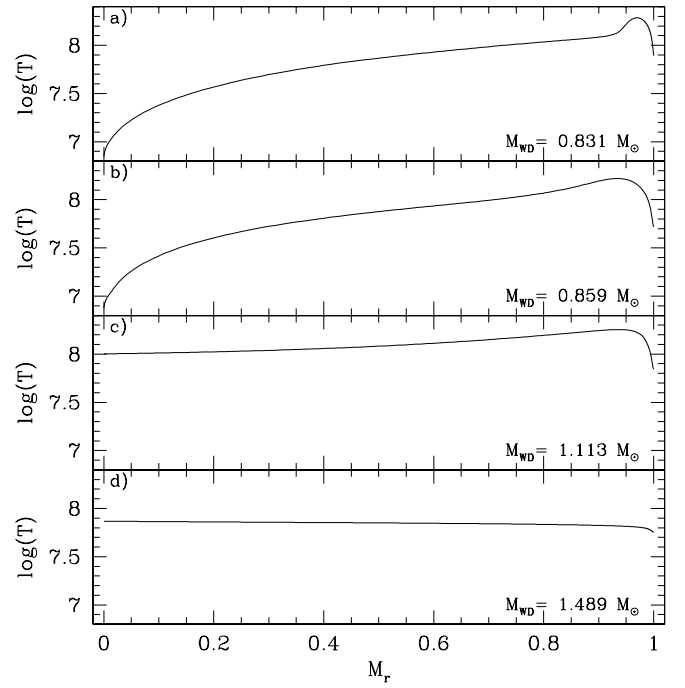


FIG. 7.—Temperature profiles for selected structures during the accretion process. (a) Occurrence of the Roche instability. (b) Beginning of the GWR-driven accretion phase. (c) One-third of the way through the GWR-driven accretion phase. (d) End of the GWR-driven accretion phase. In each panel, the total mass of the model is reported (see text) and mass fraction  $M_r/M_{\odot}$  is given along the horizontal axis.

tion. As accretion continues at the plateau rate of  $\sim 4 \times 10^{-7} M_{\odot}$ , heat diffuses steadily inward and the difference between temperatures in the deep interior and those in surface layers becomes smaller and smaller, as illustrated in Figure 7c at a time approximately one-third of the way through the GWR-controlled phase of accretion. By the end of the GWR-regulated phase, the WD structure is essentially isothermal, and after accretion effectively ceases, it begins to cool, as illustrated by the temperature profile in Figure 7d compared with the profile in Figure 7c.

In Figure 8 we report the evolution in the  $\rho$ - $T$  plane of the center of the accreting WD. During the initial constant- $\dot{M}$  phase, the innermost zones of the WD are only slightly heated by the compression produced by the increase in the mass of the WD, while expansion continues due to the increase of the angular velocity [isothermal decrease in the central density at  $\log(T) \sim 6.85$ ]. When the Roche instability occurs, the innermost regions begin to heat up because of both compression and inward thermal diffusion, while densities continue to decrease due to the increase in the angular velocity [up to  $\log(T) \sim 6.93$ ]. When the secular instability sets in and the WD starts radiating gravitational waves, temperatures in the innermost region increase dramatically [up to  $\log(T) \sim 8.0$ ] as the temperature distribution in the WD adjusts to a new equilibrium between accretion-induced heating in outer layers and the inward diffusion of heat (see Fig. 7c). After this new equilibrium is established, temperatures in the innermost regions increase at a more modest rate [up to  $\log(T) \sim 8.1$ ]. When the WD structure becomes stable again and angular momentum braking by GWR ceases, compressional heating becomes very inefficient and radiative losses from the surface cool the entire

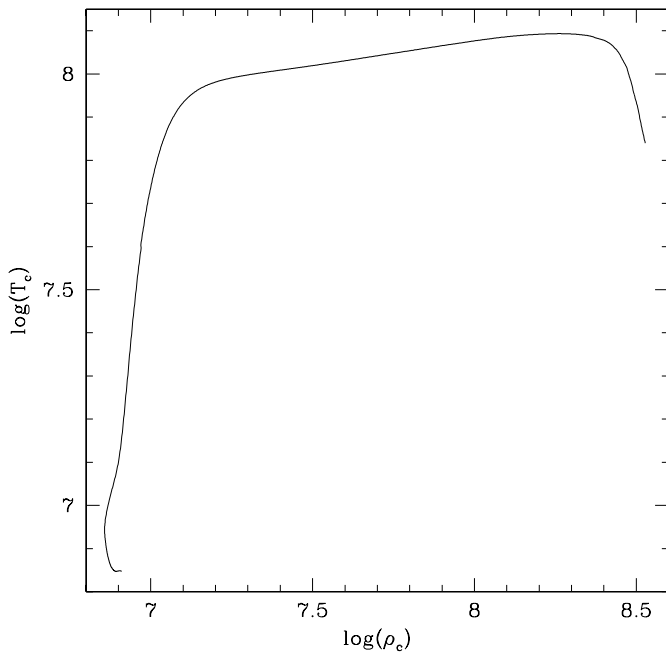


FIG. 8.—Evolution in the  $\rho$ - $T$  plane of matter at the center of the accreting WD up to the end of the GWR-driven accretion phase (see text).

WD structure, thus producing the final decrease in central temperature shown [for  $\log(\rho) > 8.3$ ].

After the GWR-driven phase has ended, the accretion rate is once again determined by the requirement that the WD remains stable against the Roche instability. Thus, as discussed in § 3.2,  $\dot{M}_{\text{eff}}$  decreases monotonically. But the WD is now quite massive ( $M_{\text{WD}} \sim 1.491 M_{\odot}$ ) and is a very fast rotator ( $\omega_{\text{WD}} \sim 1.5 \text{ rad s}^{-1}$ ), so the effective rate at which angular momentum can be deposited by accreted matter is very small. In consequence, accretion may, from this moment on, be neglected.

In the real world, matter probably continues to be deposited onto the WD along the equatorial disk, flows to the poles, and then returns ultimately to what remains of the thick disk. We can envision the WD being embedded in a viscous medium that acts to brake the rotation of the WD, angular momentum, and energy being transferred from the WD to the disk through the action of viscous forces. Because of our poor knowledge of the physical mechanisms that determine viscosity, the efficiency of the envisioned braking process is not easy to evaluate. We have modeled it by employing equation (3), replacing  $\tau_{\text{GWR}}$  with a viscous timescale  $\tau_{\text{vis}}$ . According to Ma (2002), the braking timescale can vary from  $10^4$  to  $10^8$  yr, so we have performed several numerical experiments, varying  $\tau_{\text{vis}}$ .

The results are displayed in Figure 9, where solid curves describe the evolution in the  $\rho$ - $T$  plane of matter at the centers of models with different values of  $\tau_{\text{vis}}$ , as labeled in the figure. The long-dashed curve describes matter near the center at the beginning of the experiments. The short-dashed ignition curve is defined by setting the neutrino loss rate equal to the carbon-burning rate.

For a very low braking efficiency ( $\tau_{\text{vis}} = 10^8$  yr), the heating of the WD structure is not efficient and, after a transient, the central temperature adopts an almost constant value, while the central density continues to increase. The

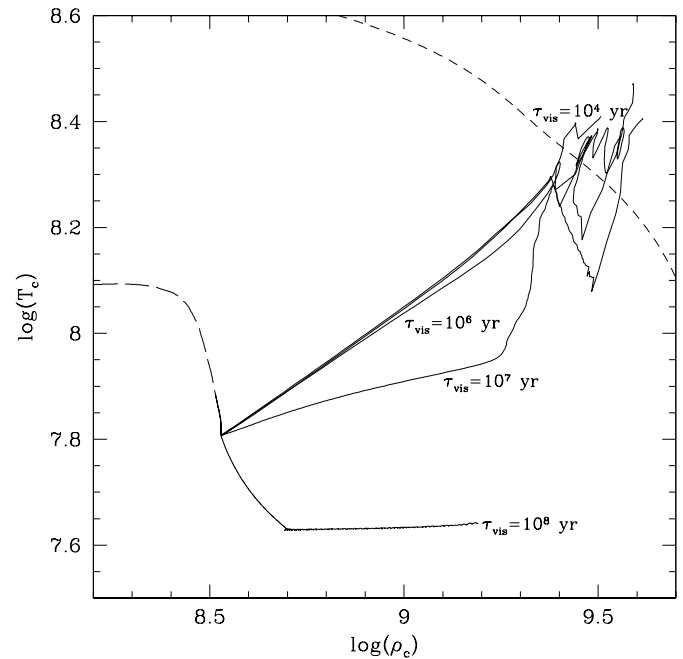


FIG. 9.—Evolution in the  $\rho$ - $T$  plane of matter at the center of the spinning-down WD after the end of the GWR-driven accretion phase. Attached to each line is the corresponding value of  $\tau_{\text{vis}}$  (see text).

computation has been halted, since our equation of state does not cover the full range of parameters needed. Nevertheless, extrapolating the behavior depicted in Figure 9, we suggest that, with adequate input physics, this model will ignite carbon burning under pycnonuclear conditions.

For larger braking efficiencies (smaller values of  $\tau_{\text{vis}}$ ), the global behavior of the model WD is completely different. The compression induced by the loss of angular momentum produces interior heating up to the moment when the  $\rho$ - $T$  curve defined by matter at the center crosses the ignition curve and carbon-burning is ignited at the center. Exactly where this crossing occurs varies with the choice of braking efficiency. Since the value of the braking efficiency operating in the real world probably depends on the total mass of the initial DD system, some of the variations in the observed characteristics of real SNe Ia could be attributed to variations in the total mass of the progenitor DD systems. For all the explored cases, carbon ignition occurs under highly electron-degenerate conditions, so that the final outcome is a dynamic explosion.

As a final exercise, we have explored the consequences of assuming that accretion ceases when the central WD has a mass smaller than  $1.5 M_{\odot}$  but still larger than the Chandrasekhar mass for nonrotating WDs. The results are shown in Figure 10, where the solid curves describe the evolution in the  $\rho$ - $T$  plane of matter at the centers of models of three different total masses (1.4, 1.43, and  $1.46 M_{\odot}$ ) and four different braking timescales, as labeled inside each panel. In each panel, the smaller the WD mass, the smaller the density at which the corresponding evolutionary track departs from the long-dashed locus. In all cases, carbon burning is ignited at the center. For large braking efficiencies ( $\tau_{\text{vis}} \leq 10^6$  yr), models experience ordinary thermonuclear ignition of carbon, while for small efficiencies, the ignition is pycnonuclear.

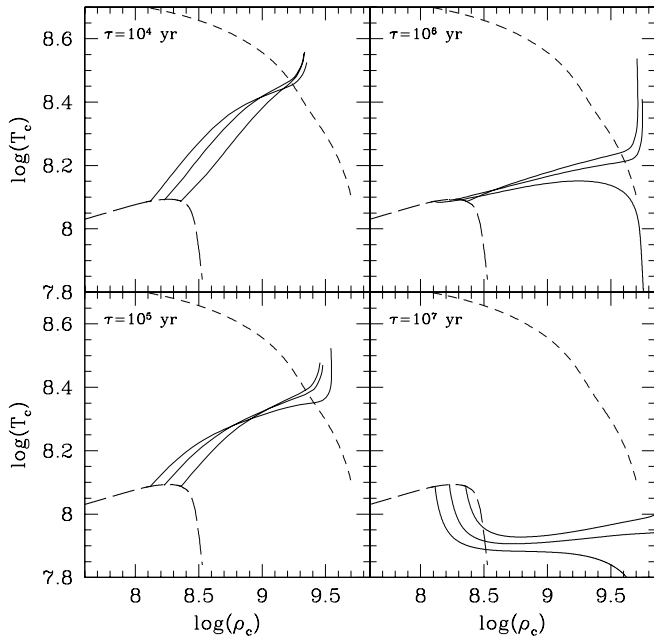


FIG. 10.—Evolution in the  $\rho$ - $T$  plane of matter at the centers of spinning-down WDs with different braking efficiencies, as labeled inside the panels. *Short-dashed lines*: Ignition curve. *Long-dashed line*: Matter near the WD center at the end of the accretion process. *Solid lines*: Density and temperature of matter at the center for WD masses of 1.4, 1.43, and 1.46  $M_{\odot}$ ; the smaller the mass of the WD, the smaller is the density at which the evolution begins.

#### 4. FINAL REMARKS

In the present work, we have explored the effect of rotation on the evolution of a double degenerate system that undergoes a merger. In our analysis, we have included the effect of rotation both during the premerger evolution of the DD system and during the accretion phase. For the adopted value of the mass ratio of the DD system, the angular velocity of the WDs at merging is very large ( $\omega = 0.177 \text{ rad s}^{-1}$ ).

We have shown that an accreting WD in a DD system can increase its mass up to and beyond  $M_{\text{Ch}}$ , even if the initial value of  $\dot{M}$  is so large that, if accretion were to continue at this rate, off-center ignition of carbon would occur. Because of rotation, a Roche instability arises early on in the accretion phase, and the effective accretion rate adopts a value determined by  $\omega_{\text{WD}} = \omega_{\text{cr}}$ , independent of the initial accretion rate. As evolution progresses, the WD spins ever faster and a secular instability sets in when the rotational energy of the WD reaches  $\sim 0.14$  of its gravitational binding energy. The WD structure then develops a quadrupole moment and emits GWR, which acts to tightly control the further evolution of the accretion process.

Two crucial points are to be emphasized:

1. Both (a) the decrease of  $\dot{M}_{\text{eff}}$  from an initial accretion rate expected to be close to the Eddington accretion rate and (b) the emission of GWR by the WD are direct consequences of the assumption that the accreting WD is rotating. These results are inevitable consequences; they are not artifacts imposed to adjust the accretion rate in such a way as to artificially achieve central ignition.

2. The results we have obtained are independent of the initial value of  $\dot{M}$ . This conclusion has been checked in detail in the present work, but it also follows from the

results of Paper I (see § 4.2), where it is shown that, for initially large values of the angular velocity, the Roche instability occurs for accretion rates in the range  $10^{-8} M_{\odot} \text{ yr}^{-1} \leq \dot{M} \leq 10^{-5} M_{\odot} \text{ yr}^{-1}$ .

Point (2) demonstrates that WD evolution up to the onset of the Roche instability is independent of processes whereby the disk loses angular momentum by means other than by transfer to the WD. On the other hand, the occurrence of the gravitational instability, with the consequent deformation of the white dwarf into a structure with a quadrupole moment, initiates a new accretion regime which is completely driven by the WD behavior. In fact, at the critical surface defined by the condition  $F_{\text{grav}} = F_{\text{rot}}$ , the specific angular momentum of the WD is equal to that of the disk so that frictional torques, which are important in determining the evolution of the inner layers of the disk, play a negligible role in the evolution of the matter in contact with the WD. As a consequence, no mass transfer takes place. At this point, the external layers of the WD contract due only to evolutionary effects (thermal inward diffusion of heat), thus producing the increase of the gravitational force at the contact surface. Hence, matter surrounding the accreting structure is gravitationally caught in such a way as to evolve toward a new equilibrium condition.

For the specific model we have studied in detail, the accretion process naturally comes to an end when the total mass of the WD reaches 1.491  $M_{\odot}$ . At this stage, since it is embedded in a viscous medium, the WD continues to lose angular momentum. Compressional heating takes place as the WD spins down, and since it is more massive than the Chandrasekhar mass limit for nonrotating WDs, carbon is ultimately ignited at the center. We have explored the possible final outcomes as a function of the efficiency of angular momentum braking and have found that, regardless of the details, central carbon burning ignites under highly electron-degenerate conditions. The effect of assuming different braking timescales is a variation in the central temperature and density at which the thermonuclear runaway occurs, an ordinary thermonuclear explosion occurring for the shortest assumed timescales and a pycnonuclear explosion occurring for the largest.

In closing, we note that in our experiments, a time of approximately  $10^6 \text{ yr}$  is required for the central WD to accrete enough mass to achieve explosive conditions at the center. The referee has made the interesting suggestion that mass loss from the disk to outer space could occur sufficiently rapidly that the disk disappears before the WD has accreted the requisite amount of mass. This is a valid point that deserves investigation by those proficient in disk physics. Our suspicion is that wind mass loss from the disk is not of major importance in the context of our problem. Mass-loss rates characterizing winds from the hottest and most luminous central stars of planetary nebulae are only of the order of a few times  $10^{-8} M_{\odot} \text{ yr}^{-1}$ . The luminosity of the accreting WD in our problem is several orders of magnitude smaller than that of the hottest WDs in planetary nebulae and only a fraction of this luminosity is absorbed by the disk. The luminosity generated by the release of gravitational potential energy in the disk is also smaller than the luminosity of the hottest central stars in planetary nebulae. Thus, we guess that the wind emitted by the disk in the DD scenario is insufficient by 2 orders of magnitude to affect our conclusions.

## REFERENCES

- Benz, W., Cameron, A. G. W., Press, W. H., & Bowers, R. L. 1990, *ApJ*, 348, 647
- Bragaglia, A., Greggio, L., Renzini, A., & D'Odorico, S. 1990, *ApJ*, 365, L13
- Cassisi, S., Iben, I., Jr., & Tornambé, A. 1998, *ApJ*, 496, 376
- Chandrasekhar, S. 1970, *Phys. Rev. Letters*, 24, 611
- Friedman, J. L., & Schutz, B. F. 1975, *ApJ*, 199, L157
- Hachisu, I., Kato, M., & Nomoto, K. 1996, *ApJ*, 470, L97
- Hernanz, M., Isern, J., Canal, R., Labay, J., & Mochkovitch, R. 1988, *ApJ*, 324, 331
- Hillebrandt, W., & Niemeyer, J. C. 2000, *ARA&A*, 38, 191
- Hoyle, F., & Fowler, W. A. 1960, *ApJ*, 132, 565
- Iben, I., Jr., & Tutukov, A. V. 1984a, in *Stellar Nucleosynthesis*, ed. C. Chiosi & A. Renzini (Dordrecht: Reidel), 181
- . 1984b, *ApJS*, 54, 335
- . 1991, *ApJ*, 370, 615
- Iben, I., Jr., Tutukov, A. V., & Fedorova, A. V. 1998, *ApJ*, 503, 344
- Isern, J., Labay, J., Hernanz, M., & Canal, R. 1983, *ApJ*, 273, 320
- Koen, C., Orosz, J. A., & Wade, R. A. 1998, *MNRAS*, 300, 695
- Ma, F. 2002, *Gen. Rel. Grav.*, 34, 1319
- Nomoto, K. I. 1982a, *ApJ*, 253, 798
- . 1982b, *ApJ*, 257, 780
- Nomoto, K. I., & Iben, I., Jr. 1985, *ApJ*, 297, 531
- Piersanti, L., Cassisi, S., Iben, I., Jr., & Tornambé, A. 1999, *ApJ*, 521, L59
- . 2000, *ApJ*, 535, 932
- Piersanti, L., Cassisi, S., & Tornambé, A. 2001, *ApJ*, 558, 916
- Piersanti, L., Gagliardi, S., Iben, I., Jr., & Tornambé, A. 2003, *ApJ*, 583, 885
- Rasio, F. A., & Shapiro, S. L. 1995, *ApJ*, 438, 887
- Robinson, E. L., & Shafter, A. W. 1987, *ApJ*, 332, 296
- Saffer, R. A., Livio, M., & Yungelson, L. R. 1998, *ApJ*, 502, 394
- Saio, H., & Nomoto, K. I. 1985, *A&A*, 150, L21
- . 1998, *ApJ*, 500, 388
- Sutantyo, W. 1974, *A&A*, 35, 251
- Tassoul, J. L. 1978, *Theory of Rotating Stars*, Princeton Series in Astrophysics (Princeton: Princeton Univ. Press)
- Tornambé, A. 1989, *MNRAS*, 239, 771
- Tutukov, A. V., & Yungelson, L. R. 1979, *Acta Astron.*, 23, 665
- Webbink, R. F. 1984, *ApJ*, 277, 355
- Webbink, R. F., & Iben, I., Jr. 1988, in *Faint Blue Stars*, ed. A. G. Davis Philip, D. S. Hayes, & J. W. Liebert (Schenectady: L. Davis), 445
- Whelan, J., & Iben, I., Jr. 1973, *ApJ*, 186, 1007
- Woosley, S. E., & Weaver, T. A. 1994, *ApJ*, 423, 371